

# Terahertz polarization beam splitter based on photonic crystal and multimode interference\*

LIU Han (刘汉) and LI Jiu-sheng (李九生)\*\*

Centre for Terahertz Research, China Jiliang University, Hangzhou 310018, China

(Received 20 June 2014)

©Tianjin University of Technology and Springer-Verlag Berlin Heidelberg 2014

We design a compact terahertz (THz) polarization beam splitter. Both plane wave expansion method and finite-difference time-domain method are used to calculate and analyze the characteristics of the proposed device. The designed polarization beam splitter can split TE-polarized and TM-polarized THz waves into different propagation directions. The simulation results show that the extinction ratios are larger than 18.36 dB for TE polarization and 13.35 dB for TM polarization in the frequency range from 1.86 THz to 1.91 THz, respectively. The designed polarization beam splitter has the advantages of small size and compact structure with a total size of 4.825 mm×0.400 mm.

**Document code:** A **Article ID:** 1673-1905(2014)05-0325-4

**DOI** 10.1007/s11801-014-4119-2

Terahertz (THz) wave refers to the wave with frequency from 0.1 THz to 10 THz, which has attracted extensive attention and investigation due to its potential applications in a variety of areas, such as physics, chemistry, electronic information, biology, free space communication and materials science<sup>[1]</sup>. These applications have dramatically accelerated the study of THz functional devices, including switches<sup>[2]</sup>, filters<sup>[3]</sup>, modulators<sup>[4,5]</sup> and splitters<sup>[6]</sup>. At present, the development of an efficient control of THz wave power splitter is still challenging. But, over the past decades, most of the polarization beam splitter researches focus on optical frequency region. According to the device structure, the polarization beam splitters can be roughly divided into four types of Mach-Zehnder interferometer structure<sup>[7]</sup>, directional coupler structure<sup>[8]</sup>, photonic crystal structure<sup>[9]</sup> and multimode interference structure<sup>[10]</sup>. However, among these polarization beam splitters, some devices have very long size, while others have relatively complex structure. Fortunately, photonic crystals provide a new opportunity for this critical issue due to the existence of photonic band gap. Photonic crystals have been proven both theoretically and experimentally to be an effective way to perfectly transmit and flexibly control electromagnetic wave.

In this paper, we propose a novel compact THz polarization beam splitter by combining photonic crystal and multimode interference structure. In the proposed scheme, the power splitter structure consists of multimode interference section and photonic crystal. Both the plane wave expansion method and finite-difference time-domain method are used to analyze and simulate

the characteristics of the proposed device. The polarization extinction ratio is more than 13 dB, and the efficient frequency range covers the band from 1.86 THz to 1.91 THz. By using the internal photonic crystal structure, the total size of the polarization beam splitter is reduced dramatically. Furthermore, the proposed THz polarization beam splitter made of single silicon material is suitable for the integration with other THz wave devices.

The schematic diagram of the structure of the proposed polarization beam splitter is shown in Fig.1. In Fig.1, part I is the input waveguide, and part II is the multimode interference section in which a photonic crystal structure is located in the middle region. Parts III and IV are the output waveguides for TM polarization and TE polarization. The structure is made of a high-resistivity silicon material due to its transparency and low absorption in THz region, and its refractive index is 3.42. The two-dimensional silicon photonic crystal is high-resistivity silicon substrate with air holes in triangular lattice. The radius of the photonic crystal air column is set to be  $r=0.26a$ .

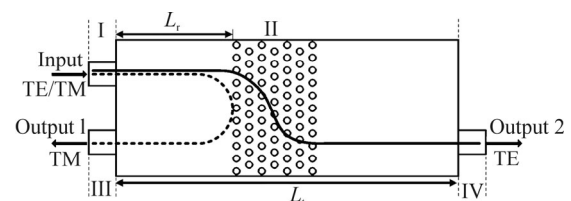


**Fig.1 Schematic diagram of structure of the THz polarization beam splitter**

When a single mode electromagnetic wave is input

\* This work has been supported by the National Natural Science Foundation of China (Nos.61379024 and 61131005), and the Zhejiang Provincial Outstanding Youth Foundation (No.LR12F05001).

\*\* E-mail:lijsh2008@126.com

into a multimode waveguide, the total field  $\psi(x, z)$  can be calculated by the superposition of exited modes as follows<sup>[11,12]</sup>

$$\psi(x, z) = \sum_{n=0}^{p-1} c_n \varphi_n(x) e^{-i\beta_n z}, \quad (1)$$

where  $c_n$  is field excitation coefficient,  $p$  is the number of guide modes, the subscript  $n$  denotes the order of the mode,  $\varphi_n(x) e^{-i\beta_n z}$  is modal field distribution, and  $\beta_n$  is propagation constant of the  $n$ th mode. For the direct and mirrored images, which are reproduced at  $z=L_d$  and  $z=L_m$  respectively, the positions can be expressed as

$$\beta_n L_d = 2k\pi, \quad k = 1, 2, 3, \dots, \quad (2)$$

$$\beta_n L_m = 2k\pi, \quad k = 1, 2, 3, \dots, \quad \beta_n \text{ is even mode}, \quad (3)$$

$$\beta_n L_m = (2k-1)\pi, \quad k = 1, 2, 3, \dots, \quad \beta_n \text{ is odd mode}. \quad (4)$$

Fig.2 shows the TE and TM band diagrams of the photonic crystal. By using plane wave expansion method, we find that there is an absolute photonic band gap for TM polarization in the frequency range from  $0.210(a/\lambda)$  to  $0.247(a/\lambda)$ , while there is no band gap for TE polarization. The photonic crystal exhibits a high transmission for the TE polarization but a large reflection for TM polarization. When both the TE polarization and the TM polarization THz waves are input into the multimode interference section and transmitted to the photonic crystal, it can be noted that the TE polarization THz wave is transmitted through the photonic crystal region, while TM polarization THz wave is reflected, and then they are separated into two output waveguides. Assuming that  $T$  is transmission coefficient and  $R$  is reflection coefficient, the backward propagating field  $\psi_1(x, 0)$  at output1 and forward propagating field  $\psi_2(x, L_t)$  at output2 can be given by<sup>[13]</sup>

$$\psi_1(x, 0) = R \cdot \sum_n c_n \varphi_n(x) \exp\left[-j \frac{n(n+2)\pi}{3L_\pi} 2L_t\right], \quad (5)$$

$$\psi_2(x, L_t) = T \cdot \sum_n c_n \varphi_n(x) \exp\left[-j \frac{n(n+2)\pi}{3L_\pi} L_t\right], \quad (6)$$

where  $L_t$  is the distance between the start of the multimode interference section and the beginning of the photonic crystal region, and  $L_t$  is the total length of the multimode interference section. Here,  $L_t$  and  $L_r$  are set to be  $L_t = L_d^{TM}$  and  $L_r = L_m^{TE} / 2$ , where  $L_d^{TM}$  is the first direct image position for TM polarization, while  $L_m^{TE}$  is the first mirrored image position for TE mode.  $L_\pi$  is the length of the lowest two order modes, which is expressed as

$$L_\pi = \frac{\pi}{\beta_0 - \beta_1} \approx \frac{4n_r W_c^2}{3\lambda_0}, \quad (7)$$

where  $n_r$  is the effective refractive index of the multimode interference coupler's material,  $W_c$  is the width of the photonic crystal region, and  $\lambda_0$  is the incident wavelength of the THz wave.

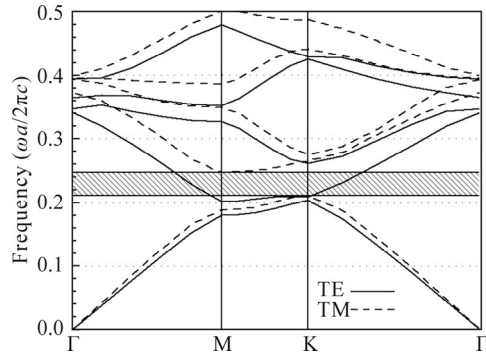
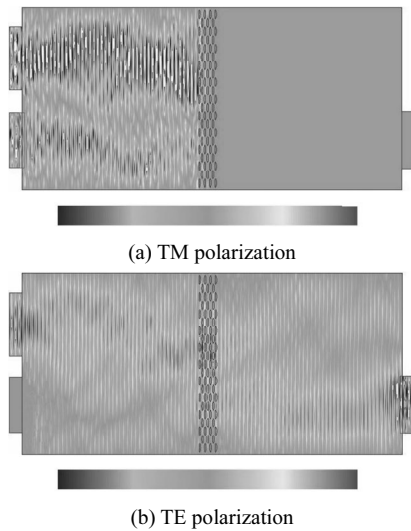


Fig.2 Band diagrams of the photonic crystal

In order to ensure the high quality of self-imaging, the width of multimode interference coupler should guarantee that the multimode waveguide needs to support enough guided modes. Here, the width of multimode interference section is set to be  $400 \mu\text{m}$ , the length and width of the input and output waveguides are set to be  $125 \mu\text{m}$  and  $200 \mu\text{m}$ , respectively. According to Eqs.(1)–(7), we obtain  $L_\pi^{TE} = 4825 \mu\text{m}$  and  $L_\pi^{TM} = 4485 \mu\text{m}$ , respectively. Then, we can also obtain  $L_t = L_\pi^{TE} = 4825 \mu\text{m}$  and  $L_r = L_\pi^{TM} / 2 = 2242.5 \mu\text{m}$ . The photonic crystal structure is made up of seven column air holes. The working frequency point is set to be  $0.232(\omega a/2\pi c)$ , the lattice constant is assumed to be  $a=37 \mu\text{m}$ , and the corresponding working frequency is  $f=1.881 \text{ THz}$ . Fig.3 shows the steady-state electric field distributions for both TE and TM polarizations obtained by finite-difference time-domain method. According to Fig.3(a), it can be seen that the TM polarization THz wave is reflected by the photonic crystal with high reflection efficiency and finally collected by output1. For TE polarization THz wave, according to Fig.3(b), it is transmitted through the photonic region with high transmission efficiency and finally collected by output2. The simulation results show that the input THz wave can be successfully split into output1 with TM polarization and output2 with TE polarization. Furthermore, the simulated propagation pattern of electric field agrees well with the theoretically calculated length, where the positions of TM polarization direct images and TE mirrored images satisfy Eqs.(2)–(4). Fig.4 shows the cross section of steady-state electric field distributions, and the location of the cross section is selected at the fifth column of air holes in the photonic crystal region. It can be noted that the TM polarization THz wave can't be transmitted through the fifth column of air holes, while TE polarization THz wave can, with high transmission efficiency.

The normalized output power transmittance spectra of two output branches are shown in Fig.5. It can be seen from Fig.5 that insertion losses of TE and TM polarization are 2.23 dB and 2.02 dB in the frequency range from 1.86 THz to 1.90 THz, respectively. In order to investigate the structure quantitatively, we numerically determine the power flows of the two output waveguides by simulation using finite-difference time-domain method. For TM and TE polarization, the polarization extinction

ratios of transmission are defined as  $-10\log(T_{TM}/T_{TE})$  and  $-10\log(R_{TE}/R_{TM})$ , respectively. Fig.6. shows the extinction ratios for TE and TM polarization. The polarization extinction ratio of the transmission for TE polarization is larger than 18.36 dB, whereas the corresponding polarization extinction ratio of the reflection for TM polarization is larger than 13.35 dB. According to the proposed scheme, the total device size of our polarization beam splitter is only  $4.825\text{ mm}\times 0.400\text{ mm}$ .



**Fig.3 Steady-state electric field distributions at  $f=1.881\text{ THz}$**

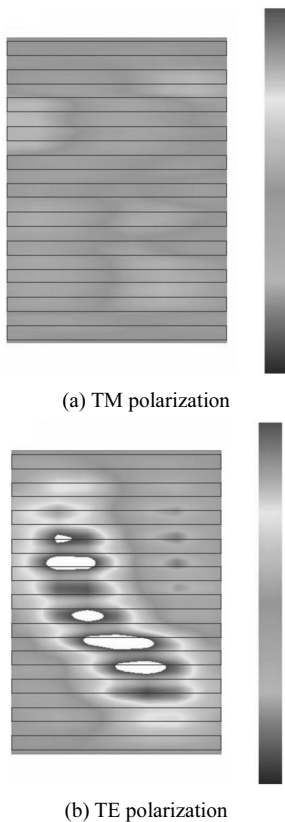
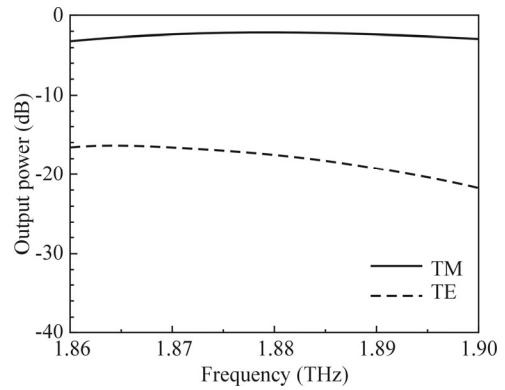
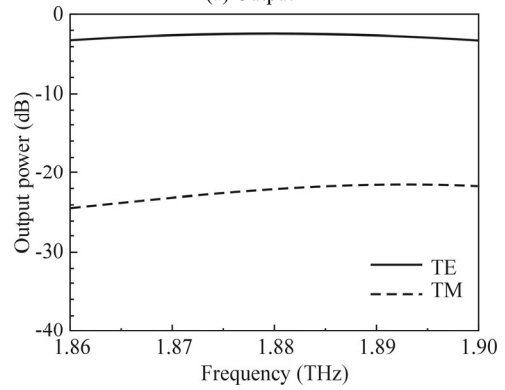


**Fig.4 Steady-state electric field distributions in cross section at  $f=1.881\text{ THz}$**



(a) Output1



(b) Output2

**Fig.5 Normalized output power of the two branches**

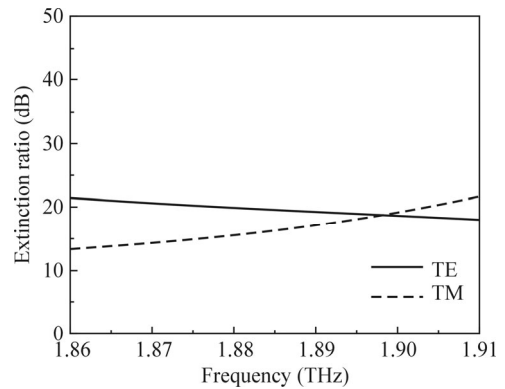


**Fig.6 Polarization extinction ratios of the proposed THz wave polarization beam splitter**

A compact THz wave polarization beam splitter combining multimode interference coupler and photonic crystal structure is proposed and numerically demonstrated. The simulation results show that the extinction ratios are larger than 13 dB for both TE and TM polarization in the frequency range from 1.86 THz to 1.91 THz. Numerical simulation results agree well with the theoretical calculation. Besides simplicity and small size, this novel THz wave polarization beam splitter can work in a broad frequency range, and it can be fabricated on a wafer and integrated with other planar THz-wave circuits.

**References**

[1] YANG Zhen-gang, LIU Jin-song and WANG Ke-jia, Journal

- of Optoelectronics-Laser **24**, 1158 (2013). (in Chinese)
- [2] Yinghao Yuan, Jian He, Jinsong Liu and Jianquan Yao, Applied Optics **49**, 6092 (2010).
- [3] Mingzhi Lu, Wenzao Li and Elliott R. Brown, Optics Letters **36**, 1071 (2011).
- [4] Jie Shu, Ciyuan Qiu, Victoria Astley, Daniel Nickel, Daniel M. Mittleman and Qianfan Xu, Optics Express **19**, 26666 (2011).
- [5] LI Zhong-yang, YAO Jian-quan, XU De-gang, BING Pi-bin and ZHONG Kai, Journal of Optoelectronics-Laser **23**, 425 (2012). (in Chinese)
- [6] Jiu-sheng Li, De-gang Xu and Jian-quan Yao, Applied Optics **49**, 4494 (2010).
- [7] Chen X., Qiang Z., Zhao D., Wang Y., Li H., Qiu Y. and Zhou W., Optics Communications **284**, 490 (2011).
- [8] Xiaowei Guan, Hao Wu, Yaocheng Shi, Lech Wosinski and Daoxin Dai, Optics Letters **38**, 3005 (2013).
- [9] She J., Forsberg E., Ao X. Y. and He S. L., Journal of Optics A: Pure and Applied Optics **8**, 345 (2006).
- [10] Kwong D., Zhang Y., Hosseini A., Liu Y. and Chen R. T., Electronics Letters **46**, 1281 (2010).
- [11] Hyun-Jun Kim, Insu Park, Beom-Hoan O, Se-Geun Park, El-Hang Lee and Seung-Gol Lee, Optics Express **12**, 5625 (2004).
- [12] Yao Zhang, Zhangjian Li and Baojun Li, Optics Express **14**, 2679 (2006).
- [13] Soldano L. B. and Pennings E. C. M., Journal of Light-wave Technology **13**, 615 (1995).